

- ⁴H. R. Glyde, Phys. Rev. **180**, 722 (1969).
⁵C. P. Flynn, Phys. Rev. Lett. **35**, 1721 (1975).
⁶G. Verdan, R. Rubin, and W. Kley, in *Proceedings of the Fourth IAEA Symposium on Neutron Inelastic Scattering, Copenhagen, Denmark, 1968* (International Atomic Energy Agency, Vienna, Austria, 1968), Vol. 1, p. 223.
⁷J. H. Weiner and Y. Partom, Phys. Rev. **187**, 1134 (1969).
⁸J. A. Sussman and Y. Weissman, Phys. Status Solidi (b) **53**, 419 (1972).
⁹Yu. Kagan and M. I. Klinger, J. Phys. C **7**, 2791 (1974).
¹⁰C. P. Flynn and A. M. Stoneham, Phys. Rev. B **1**, 3966 (1970); A. M. Stoneham, Ber. Bunsenges. Phys. Chem. **76**, 816 (1972).
¹¹T. Holstein and L. Friedman, Phys. Rev. **165**, 1019 (1968); E. O. Kane, Phys. Rev. **119**, 40 (1960).
¹²T. F. Soules and C. B. Duke, Phys. Rev. B **3**, 262 (1971).
¹³R. Kubo, J. Phys. Soc. Jpn. **12**, 570 (1957).
¹⁴T. Holstein, Ann. Phys. (N.Y.) **8**, 325, 343 (1959).
¹⁵D. Emin, Adv. Phys. **24**, 305 (1975), and to be published.
¹⁶W. Magnus, F. Oberhettinger, and R. Soni, *Formulas and Theorems for the Special Functions of Mathematical Physics* (Springer, Berlin, 1966).
¹⁷R. Zwanzig, in *Annual Review of Physical Chemistry*, edited by H. Eyring, C. Christensen, and H. Johnston (Annual Review, Palo Alto, Calif., 1965), p. 67.

Quasiparticle-Injection-Induced Superconducting Weak Links*

Ting-wah Wong, J. T. C. Yeh,[†] and D. N. Langenberg

Department of Physics and Laboratory for Research on the Structure of Matter, University of Pennsylvania, Philadelphia, Pennsylvania 19174

(Received 3 May 1976)

Superconducting weak links are studied in which the weak region is created by locally driving the superconductor out of equilibrium using an independent source of quasiparticles. The characteristics of these weak links can be varied electrically or optically at any temperature below T_c . A simple model which describes the dependence of weak-link critical current on quasiparticle-injection rate is presented.

A common feature of all superconducting weak links is a localized region of depressed superconducting order parameter separating two superconductors. The size of the localized weak region must be comparable with or smaller than a characteristic length of the superconductor, generally supposed to be the temperature-dependent coherence length $\xi(T)$. This condition imposes rather severe constraints on the fabrication and operation of weak links. The link dimensions must be at the micrometer level and desired operating characteristics can often be achieved only within a rather restricted temperature interval. We report here some initial experimental observations on a new class of weak links in which the weak region is not a result of a fabrication process, but is created by locally driving the superconductor out of equilibrium using a source of quasiparticles which is independent of the primary weak-link circuit.¹ The characteristics of these weak links can be electrically or optically varied at any temperature below T_c . We also present a simple model, based on current understanding of the non-equilibrium superconductor, which accounts for

the dependence of the weak-link critical current on quasiparticle-injection rate.

Consider a narrow thin-film strip of superconductor, a microbridge of width W . Suppose it is possible by some means to inject or create excess quasiparticles over a length L of the microbridge. The resulting excess quasiparticle density will be position dependent, varying slowly with L and falling to zero outside L in a distance of the order of the quasiparticle diffusion length $\lambda = (v_{qp} l \tau_{eff}/3)^{1/2}$. Here v_{qp} is an average quasiparticle velocity approximately equal to the Fermi velocity, l is the quasiparticle elastic scattering mean free path, and τ_{eff} is a characteristic quasiparticle relaxation time, probably the effective quasiparticle-recombination time. The excess quasiparticles will depress the superconducting order parameter over some distance $\Lambda \sim L + 2\lambda$, creating a weak link if Λ is sufficiently small and the depression sufficiently strong. The characteristics of this weak link, e.g., the critical current, depend basically on Λ and on Δ_{min} , the gap parameter at its minimum within L . These parameters in turn depend in a rather complicated

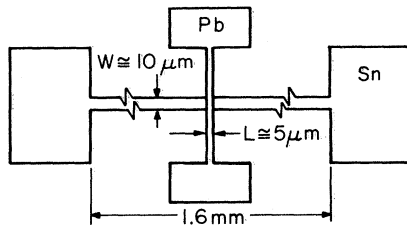


FIG. 1. Quasiparticle-injection weak-link configuration (not to scale).

way on the rate of injection or creation of quasiparticles.

We have most extensively studied quasiparticle-injection weak links in the configuration shown in Fig. 1. It shows a thin-film Sn microbridge about 1.6 mm long, 10 μm wide, and 600 to 1000 \AA thick, crossed by a Pb strip about 5 μm wide which is separated from the microbridge by a tunnel barrier formed by thermal oxidation or by glow-discharge oxidation. The critical-current densities of our tunnel junctions ranged from ~ 10 to $\sim 400 \text{ A cm}^{-2}$. Pb was used for the tunnel-injection electrode to ensure that it remained superconducting over the required range of injection currents. The injection current was divided equally between the two halves of the microbridge to ensure a symmetric distribution of quasiparticles in the injection region and to eliminate any injection-current contribution to the measured current-voltage (I - V) characteristics of the microbridge. Four-terminal measurements of both the injection tunnel junction and microbridge I - V characteristics were made over the bath-temperature range 1.3 to 4.2 K. The background ambient magnetic field was less than 1 mG.

Figure 2 shows the variation with injection current I_J of the I - V characteristic of such a tunnel-injection weak link at low reduced temperature. For $I_J = 0$, the critical current I_c is large (23 mA) and the I - V characteristic is strongly hysteretic. This behavior is typical of that attributed to the formation of a "hot spot" by Skocpol, Beasley, and Tinkham.² Very little change occurs for $I_J \leq 500 \mu\text{A}$. With further increase in I_J , I_c begins to decrease, but the hot-spot behavior persists down to critical currents of several milliamperes. Then the I - V characteristic begins to change toward the nonhysteretic shape generally associated with "ideal" weak links. Finally, I_c decreases to zero at $I_J = I_{J_0} = 1.232 \text{ mA}$. With further increase in I_J , the resistance of the now-normal link increases nonlinearly.

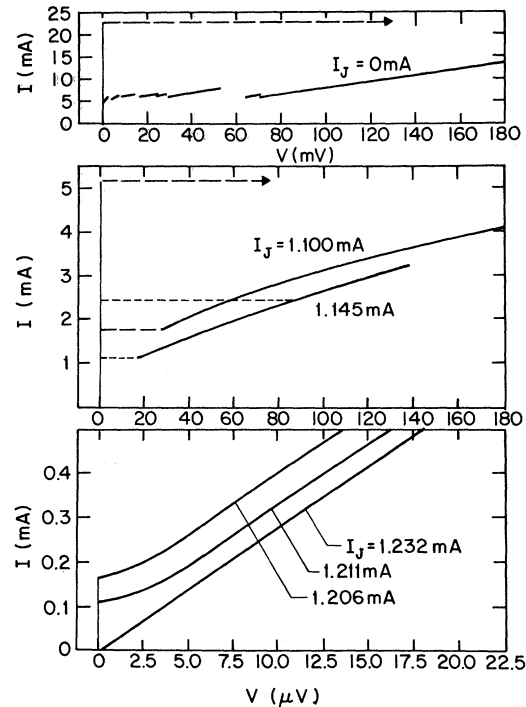


FIG. 2. Variation of weak-link I - V characteristic with tunnel-injection current. $W = 10 \mu\text{m}$; $L = 6 \mu\text{m}$; $T = 2.07 \text{ K}$. Note changes in current and voltage scales.

Some other general features of the behavior of these tunnel-injection weak links are the following: (1) For $I_c \lesssim 25 \mu\text{A}$, the critical current becomes very sensitive to an applied magnetic field. A field of about 1 G perpendicular to the film plane drives the critical current to zero. (2) For $T < T_\lambda$ and for fixed L , the injector power required to drive I_c to zero remains approximately constant as the normal-state resistance R_N of the injector junction is varied. For $T = 2 \text{ K}$, and $L = 5 \mu\text{m}$, $I_{J_0}^2 R_N \approx 8 \mu\text{W}$. The corresponding bias voltage on the injector junction ranged from about $3(\Delta_{\text{Sn}} + \Delta_{\text{Pb}})/e$ for $R_N = 5 \Omega$ to $22(\Delta_{\text{Sn}} + \Delta_{\text{Pb}})/e$ for $R_N = 240 \Omega$. (3) I_{J_0} increases continuously with decreasing temperature down to $T = T_\lambda$, where it jumps sharply by about 20% and then continues to increase. There is a corresponding sharp drop in the weak-link resistance at I_{J_0} at $T = T_\lambda$. Both effects reflect the sudden improvement in phonon removal from the weak link as T is decreased below T_λ . (4) The differential resistance of the weak link at high bias voltage decreases slowly with increasing I_J up to I_{J_0} . This appears to correspond to a shrinking of the weak region. (5) The canonical test for the presence of Josephson phase coupling in a weak link is the appearance

of steps in the I - V characteristic in the presence of rf radiation. For $I_J = 0$, we were unable to observe any such steps at X -band frequencies at any temperature significantly below T_c . With I_c tuned into the range $200 \mu\text{A} \lesssim I_c \lesssim 3 \text{ mA}$ we were able to observe rf-induced steps up to $n = 3$ at all temperatures with moderate microwave powers. The maximum observed amplitude of the $n = 1$ step was about $I_c/8$. We also frequently observed the $n = \frac{1}{2}$ and $n = \frac{3}{2}$ subharmonic steps. No steps were observed in the region $I_c \lesssim 200 \mu\text{A}$ where the I - V characteristic had the ideal-weak-link shape.

We have had several unintended opportunities to study another variant of the quasiparticle-injection weak link, one we call the "point-injection" weak link. These resulted from accidental shorting of the tunnel barrier. If such an event is not catastrophic, there is evidence³ that it often results in a single metallic conducting path through the oxide barrier only a few hundred angstroms in diameter. The injection area is then much smaller than for an undamaged barrier. The behavior of these point-injection weak links is generally similar to that of the tunnel-injection weak link. I_{J_0} is larger but the injector power at I_{J_0} is still $\sim 8 \mu\text{W}$. The weak-region size Λ appears to be significantly smaller. The rf-induced steps are considerably larger (maximum $n = 1$ step amplitude $\sim I_c/3$) and steps can be observed for $3 \text{ mA} \gtrsim I_c \gtrsim 0$.

The basic ingredients of a model which may be used in discussion of these experimental results are (1) a connection between I_J and the excess-quasiparticle distribution in the injection region, and (2) a connection between this distribution and the superconducting gap parameter or order parameter. For the first we use the phenomenological Rothwarf-Taylor equations,⁴ extended to include quasiparticle and phonon diffusion along the microbridge. The steady-state quasiparticle equation may be written as

$$D \frac{\partial^2 N}{\partial x^2} + I_0(x) - \frac{R(N^2 - N_T^2)}{(1 + \tau_\gamma/\tau_B)} = 0. \quad (1)$$

The diffusion constant $D = v_{qp}l/3$, $I_0(x)$ is the injection rate density, N is the quasiparticle number density, N_T is the thermal-equilibrium quasiparticle number density, R is the intrinsic single-quasiparticle recombination rate constant, and $(1 + \tau_\gamma/\tau_B)$ is the so-called phonon-trapping factor. Because the phonon mean free path against pair breaking is very short, it can be argued that phonon diffusion is unimportant, so that the Roth-

warf-Taylor phonon equation is unmodified.

Details of the solutions of these equations will be reported elsewhere; they include the following qualitative features. Because the recombination rate for a given quasiparticle is proportional to the quasiparticle density, when the injection rate is sufficiently high that $N > N_T$ (a regime commonly called overinjected), τ_{eff} becomes less than the near-equilibrium phonon-trapped recombination time and the quasiparticle diffusion length λ decreases. This accounts for the observed decrease in effective link length with increasing I_J . For the point-injection weak links, L may be only several hundred angstroms, and $\lambda \gtrsim L$. In this case, Λ should be strongly dependent on injection level, an expectation in accord with our observations.

For comparison with the tunnel-injection weak-link data reported here, we have used a simplified version of the above, in which the diffusion term is crudely approximated by $-\alpha I_0$, where α is the fraction of injected quasiparticles lost from the injection area by diffusion. Then Eq. (1) becomes simply

$$N = [I_0(1 - \alpha)R^{-1}(1 + \tau_\gamma/\tau_B) + N_T^2]^{1/2}. \quad (2)$$

For the second basic ingredient in our model we use Parker's modified heating or T^* model.⁵ In the T^* model it is assumed that the nonequilibrium excess quasiparticles and the phonons with energies greater than 2Δ (those emitted in quasiparticle-recombination events or absorbed in phonon pair-breaking events) are in steady-state quasithermal distributions characterized by a temperature T^* , while phonons with energies less than 2Δ are at temperature T , the ambient or bath temperature. (This overall nonthermal phonon distribution distinguishes this model from a simple heating model in which all phonons are characterized by the same temperature. The T^* model fits existing nonequilibrium-superconductor experiments rather well, while the simple heating model does not.⁵) We identify the gap parameter yielded by the T^* model for given N with Δ_{min} . (We note, however, that the T^* model assumes a spatially homogeneous system. If Λ is comparable with ξ , as it probably is in our weak links, we can have no confidence that the model is applicable, but we use it anyway for want of anything better.)

We also need a relation between I_0 and I_J . We assume that quasiparticle injection at voltage $V_J \simeq I_J R_N \gg (\Delta_{\text{sn}} + \Delta_{\text{pb}})/e$ leads to a steady-state quasiparticle distribution at temperature T^* in

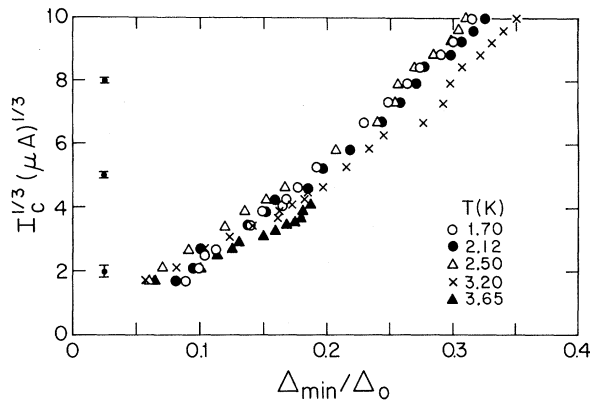


FIG. 3. Gap dependence of weak-link critical current for different bath temperatures. The error bars are typical for the indicated regions of $I_c^{1/3}$.

which the average quasiparticle energy is approximately Δ_0 , the zero-temperature zero-injection gap.⁵ Half the injector power goes to the excess quasiparticles and phonons on one side of the injector junction, with a fraction^{5,6} F appearing in the quasiparticles. With these assumptions

$$I_0 \approx \frac{1}{2} F I_J^2 R_N / \Delta_0 W L d, \quad (3)$$

where d is the film thickness.

A detailed comparison of this model with our experimental data is beyond the scope of this Letter and will be reported elsewhere. We present here just one pertinent result. The temperature or gap dependence of the critical current of weak links near T_c has been investigated by many workers.^{1,7-9} The most popular result is $I_c \propto (1-t)^{3/2}$ which, using the BCS relation $\Delta \propto (1-t)^{1/2}$, corresponds to $I_c \propto \Delta^3$. Figure 3 shows, for a variety of bath temperatures, our observed $I_c^{1/3}$ versus Δ_{min} , where we have translated the experimentally observed parameter I_J into Δ_{min} using the simplified model outlined above. The dependence of I_c on Δ_{min} is close to Δ_{min}^3 for $\Delta_{min} \lesssim 0.2\Delta_0$. In the course of the translation, we obtained a near-equilibrium phonon-trapped quasiparticle recombination time for Sn in excellent agreement with other experiments.^{10,11}

Although we have emphasized here the quasiparticle-injection weak link, the general ideas underlying its operation apply also to weak links in which the quasiparticles are created by other methods. We have made some very preliminary experiments on both photon- and phonon-induced weak links. In the latter case, the phonons were generated by a narrow ($\sim 1 \mu\text{m}$) normal-metal heater strip crossing a Sn variable-thickness bridge¹² (a short microbridge which is substan-

tially thinner than the superconducting films it connects). The heater was isolated from the bridge by a thick ($\sim 1 \mu\text{m}$) insulating film of SiO to prevent tunneling. The phonons create quasiparticles in the microbridge by pair breaking. A tunable critical current and rf-induced steps were again observed.

Our photoinjection weak link consisted of a Sn variable-thickness bridge 1000 \AA thick by $\sim 0.5 \mu\text{m}$ long by $10 \mu\text{m}$ wide, with all but the bridge region screened by an opaque silver film. The critical current of the bridge was varied using light from an ordinary high-intensity reading-lamp bulb. The rf-induced-step test in this case yielded rather spectacular results: In the absence of light, no steps could be seen. Under certain circumstances (not yet well defined, but apparently associated with minimal substrate heating) more than 50 steps extending beyond a bias voltage of 1 mV appeared.

We anticipate that further study of the several types of quasiparticle-injection-induced superconducting weak links we have described here will contribute to better understanding of both non-equilibrium phenomena in superconductors and the basic mechanisms of weak-link behavior. Their controllability may also have practical benefits.

*Supported by the Office of Naval Research.

†Present address: School of Applied and Engineering Physics, Cornell University, Ithaca, N. Y. 14853.

¹Weak coupling induced by photon irradiation has been studied theoretically by A. F. Volkov, Zh. Eksp. Teor. Fiz. **60**, 1500 (1971) [Sov. Phys. JETP **33**, 811 (1971)].

²W. J. Skocpol, M. R. Beasley, and M. Tinkham, J. Appl. Phys. **45**, 4054 (1974).

³I. K. Yanson, Zh. Eksp. Teor. Fiz. **66**, 1035 (1974) [Sov. Phys. JETP **39**, 506 (1974)].

⁴A. Rothwarf and B. N. Taylor, Phys. Rev. Lett. **19**, 27 (1967).

⁵W. H. Parker, Phys. Rev. B **12**, 3667 (1975).

⁶G. A. Sai-Halasz, C. C. Chi, A. Denenstein, and D. N. Langenberg, Phys. Rev. Lett. **33**, 212 (1974).

⁷J. Bardeen, Rev. Mod. Phys. **34**, 667 (1962).

⁸A. H. Dayem and J. J. Wiegand, Phys. Rev. **155**, 419 (1967).

⁹H. A. Notarys and J. E. Mercereau, J. Appl. Phys. **44**, 1821 (1973).

¹⁰D. N. Langenberg, *Low Temperature Physics—LT 14*, edited by M. Krusius and M. Vuorio (North-Holland, Amsterdam, 1975), Vol. V, p. 223.

¹¹J. T. C. Yeh and D. N. Langenberg, Bull. Am. Phys. Soc. **21**, 404 (1976), and to be published.

¹²K. K. Likharev, Zh. Eksp. Teor. Fiz. **61**, 1700 (1971) [Sov. Phys. JETP **34**, 906 (1972)].